

Filter-exchange PGSE NMR determination of cell membrane permeability

Ingrid Åslund*, Agnieszka Nowacka, Markus Nilsson, Daniel Topgaard

Physical Chemistry, Lund University, P.O. Box 124, SE-221 00 Lund, Sweden

ARTICLE INFO

Article history:

Received 6 May 2009

Revised 10 July 2009

Available online 17 July 2009

Keywords:

Pulsed gradient spin echo

PGSE

Membrane permeability

Intracellular lifetime

Yeast

ABSTRACT

A new PGSE NMR sequence is introduced for measuring diffusive transport across the plasma membrane of living cells. A “diffusion filter” and a variable mixing time precedes a standard PGSE block for diffusion encoding of the NMR signal. The filter is a PGSE block optimized for selectively removing the magnetization of the extracellular water. With increasing mixing time the intra- and extracellular components approach their equilibrium fractional populations. The rate of exchange can be measured using only a few minutes of instrument time. Water exchange over the plasma membrane of starved yeast cells is studied in the temperature range +5 to +32 °C.

© 2009 Elsevier Inc. All rights reserved.

1. Introduction

Water transport across the plasma membrane is a crucial process for the function of living cells [1–3]. The osmotic permeability is studied by recording how the cell size responds to a change in the chemical potential of the water in the extracellular medium [4,5], while the diffusional permeability refers to a stationary system in which there is no net flux of water. In order to resolve intra- and extracellular water in the latter case, the molecules have to be labeled in some way. The most widely used NMR methods for measuring exchange over the cell membrane rely on doping the extracellular compartment with a paramagnetic relaxation agent such as Mn^{2+} or GdDTPA^{2-} [1,6–8]. Alternatively, apparent diffusion coefficients (ADCs) as measured by pulsed gradient spin echo (PGSE) NMR can be used to separate intra- and extracellular water even without introducing extraneous substances into the sample [9–12].

The observational time scale of the PGSE experiment, the diffusion time t_d , can be varied from approximately 1 ms to 1 s. When t_d is small in comparison to the characteristic time for exchange τ , the intra- and extracellular components can be observed separately in the PGSE signal decays, i.e. spin echo amplitude E vs. diffusion weighting b . When t_d is much larger than τ , a population weighted average ADC is observed. PGSE data acquired as a function of b and t_d in the intermediate regime, $t_d \approx \tau$, can be analyzed with the Kärger model [12–16]. Unfortunately, the echo decays contain a broad, continuous range of exponential components [17], and the dependence of the echo decay shape on τ is rather weak, thus hampering accurate studies of exchange.

The Diffusion EXchange Spectroscopy (DEXSY) technique by Callaghan and Furó [18] comprises two PGSE blocks separated by a variable mixing time t_m . The gradients of each PGSE block are incremented independently and the resulting 2D data set is subjected to a 2D inverse Laplace transform (ILT) [19] yielding a 2D diffusion spectrum. Each PGSE experiment is preferably performed in the limit $t_d \ll \tau$, resulting in sharp components in the two diffusion dimensions. In analogy with the classic EXSY experiment [20], the appearance of off-diagonal peaks in the 2D spectrum is a signature of molecular exchange between the components on the time scale of t_m . Although conceptually appealing, the practical usefulness of DEXSY is limited by inordinate demands on instrument time.

In this contribution we suggest performing the DEXSY experiment in a way analogous to the Goldman–Shen experiment [21] and the double quantum filter/spin diffusion experiment by Demco and coworkers [22]. In these techniques a filter block and a mixing time, during which molecular exchange and spin diffusion takes place, precede signal detection. Differences in T_2 or linewidth are used to resolve components such as water and cellulose [23], water and ice [24], or mobile and rigid polymer segments [22]. The parameters of the filter block are optimized for removing either rigid (Goldman–Shen) or mobile (double quantum filter) components. With increasing t_m the amplitudes of the various components return to their equilibrium values.

The herein proposed Filter EXchange Spectroscopy (FEXSY) technique is obtained by replacing the first variable gradient PGSE block of the DEXSY experiment with a fixed gradient filter block optimized to remove the signal from molecules having a large ADC. This “diffusion filter” corresponds to the dipolar and double quantum filters of the spin diffusion experiments described above. In comparison to DEXSY the dimensionality of the experiment is

* Corresponding author.

E-mail address: ingrid.aslund@fkem1.lu.se (I. Åslund).

reduced, resulting in drastically shorter experiment times. The main difference with the Kärger approach is that the ADC of the various components remain independent of the experimental time scale for exchange, i.e. t_m or t_d , resulting in mathematically simpler and more robust data analysis.

The new method is demonstrated by measuring the intracellular lifetime and the cell membrane permeability of baker's yeast which is a common model system in cell biology for studies of structure and biochemical process in eukaryotic cells [25–28]. Water is crossing the plasma membrane either through the lipid bilayer or via specialized membrane proteins known as aquaporins [2,6]. Insight into the molecular mechanisms for membrane transport can be obtained from the temperature dependence of the membrane permeability [1,29]. This approach is often applied to erythrocytes, but so far not to yeast cells. As demonstrated here, the rapidity and accuracy of the FEXSY experiment allows for detailed investigations of the variation of membrane permeability with temperature.

2. Theoretical basis

The basic theory of the PGSE experiment can be found in several textbooks and reviews [14,30–33]. As shown in Fig. 1(a), the NMR signal is encoded for molecular displacements using a pair of gradient pulses with duration δ and amplitude g . The effective diffusion time t_d is defined by

$$t_d = \Delta - \delta/3 \quad (1)$$

where Δ is the time between the start of the two gradient pulses. The pulse program parameters define the diffusion sensitivity variable b through

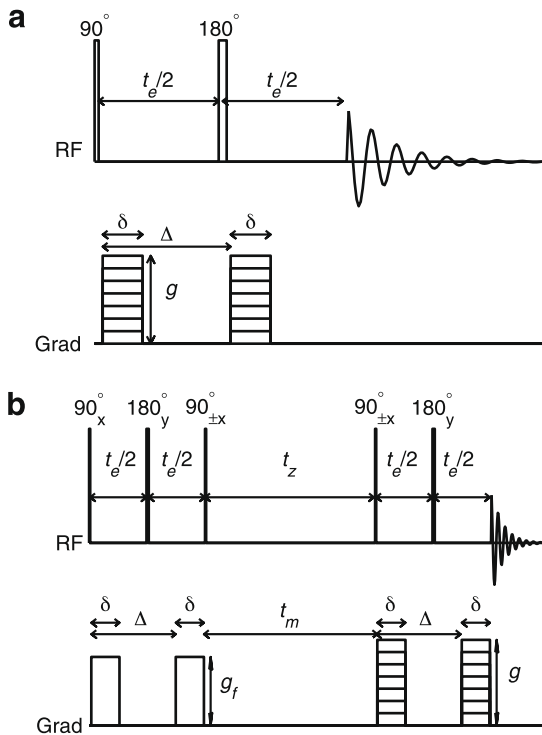


Fig. 1. Schematic timing diagrams of (a) the Pulsed Gradient Spin Echo (PGSE) and (b) the Filter EXchange Spectroscopy (FEXSY) experiments. In both figures δ is the gradient pulse duration, Δ is the time between the start of the two gradient pulses, g is the gradient strength, and t_e is the echo time during which the magnetization is subjected to T_2 -relaxation. In (b), g_f is the gradient strength during the “diffusion filter”, t_m is the mixing time, and t_z is the time interval for z -storage of the magnetization.

$$b = (\gamma g \delta)^2 (\Delta - \delta/3) \quad (2)$$

where γ is the magnetogyric ratio. In the absence of exchange processes, the normalized echo attenuation E for a cell suspension is given by [34]

$$E = f_e e^{-bD_e} + f_i e^{-bD_i} \quad (3)$$

where f is the fractional population and D the ADC. The subscripts denote the internal cell solution (i) and the extracellular medium (e). The populations are related by the condition

$$f_e + f_i = 1. \quad (4)$$

D_i is a function of t_d and δ according to [34]

$$D_i(\delta, t_d) = \frac{2}{t_d} \sum_{m=1}^{\infty} \frac{1}{\alpha_m^2 (\alpha_m^2 r^2 - 2)} \times \frac{2\alpha_m^2 D_0 \delta - 2 + 2L(\delta) + 2L(t_d + \delta/3) - L(t_d - 2\delta/3) - L(t_d + 4\delta/3)}{(\alpha_m^2 D_0 \delta)^2} \quad (5)$$

where $L(t) = e^{-\alpha_m^2 D_0 t}$, r is the cell radius, D_0 is the local self-diffusion coefficient in the intracellular compartment, and α_m are the roots of $j_1'(\alpha_m r) = 0$

in which j_1 is the 1st order spherical Bessel function. Eq. (3) is valid within the limits of the Gaussian phase distribution approximation, $\gamma G \delta \ll r^{-1}$ [34,35].

The FEXSY experiment shown in Fig. 1(b) starts with a “diffusion filter”, i.e. a PGSE block with parameters set to selectively attenuate the extracellular signal. Subsequently, molecular exchange between the intra- and extracellular compartments take place during a variable mixing time t_m . Finally, the signal is detected after a second PGSE block where the gradient is incremented as in a standard PGSE experiment. If exchange during each PGSE block can be neglected, the signal attenuation still obeys Eq. (3), but with the value of f_e modified by the filter and subsequent exchange according to standard first order reaction kinetics [36]:

$$f_e(t_m) = f_e^{eq} - [f_e^{eq} - f_e(0)] e^{-kt_m}. \quad (7)$$

In Eq. (7), f_e^{eq} is the extracellular fractional population at equilibrium and $f_e(t_m)$ the population as a function t_m . The effective exchange rate constant k is given by

$$k = k_i + k_e \quad (8)$$

where k_i and k_e are the forward and reverse exchange rates of the reaction intra \rightleftharpoons extra. Using the condition

$$f_i^{eq} k_i = f_e^{eq} k_e \quad (9)$$

and Eq. (4) yields

$$k_i = k f_e^{eq}. \quad (10)$$

The intracellular lifetime τ_i is obtained from

$$\tau_i = \frac{1}{k_i}. \quad (11)$$

In general, the diffusional permeability P for a cell can be calculated with [37]:

$$P = k_i \frac{V}{A} = k_i \frac{r}{3} \quad (12)$$

where V is the cell volume and A is the cell surface area and the second equality is valid for spherical cells.

3. Methods

3.1. Sample preparation

Fresh baker's yeast (Jästbolaget AB, Sweden) was suspended in deionized water in a weight ratio of 2:1 (yeast:water) and poured

Table 1

An overview of the parameters used. The series number are the same as indicated in Fig. 3(a).

Series	g_f/mTm^{-1}	t_m/ms	Effective t_m/ms
1	480	10.1	10.1
2	480	109.1	109.1
3	480	409.1	409.1
4	4.8	10.1	∞

into a 5 mm OD disposable NMR tube. The yeast was starved by leaving the sample in room temperature for three days. At least once every day the sample was shaken in order to release bubbles formed from yeast carbon dioxide production. Before being put into the magnet the suspension was allowed to settle under the force of gravity for ≈ 12 h, yielding a loosely packed and homogeneous sediment filling the active volume of the RF coil.

3.2. NMR experiments

NMR experiments were performed on a Bruker 200 MHz Avance-II spectrometer with a DIFF-25 gradient probe giving z -gradients up to 9.6 Tm^{-1} . For both PGSE blocks in the FEXSY experiment the following parameters were used: $\delta = 5.0 \text{ ms}$, $t_d = 7.4 \text{ ms}$, and $t_e = 16.2 \text{ ms}$. The diffusion encoding gradient g was incremented from 0.024 to 2.4 Tm^{-1} in 16 logarithmically spaced steps. Four combinations of g_f and t_m were used as reported in Table 1. Series 4, with very small values of both g_f and t_m , can be regarded as a standard PGSE experiment which is equivalent to a FEXSY experiment with $t_m = \infty$. A spoiler gradient with duration 5.0 ms and strength 96.3 mTm^{-1} was inserted in the beginning of the t_z delay. The entire data set was recorded in slightly less than 7 min when using the minimum two step phase cycle and 2 s recycle delay.

FEXSY data were acquired for temperatures from 5.0 to $32.0 \text{ }^\circ\text{C}$ using $1.0 \text{ }^\circ\text{C}$ increment and 60 s equilibration after reaching a stable temperature (within $0.1 \text{ }^\circ\text{C}$).

4. Results and discussion

4.1. Choosing experimental parameters

In order to efficiently resolve the intra- and extracellular components of the PGSE signal decay, the experimental parameters should be chosen in such a way that the difference between D_e and D_i is maximized. Previous investigations of yeast have shown that the extracellular component obeys Gaussian diffusion statistics, while the intracellular one displays the characteristics of restricted diffusion such as decreasing ADC with increasing t_d and δ [9,34]. The resolution is thus improved by using large values for t_d and δ . On the other hand, the mathematically simple analysis of the two component exchange relies on negligible molecular exchange during each PGSE block of the FEXSY experiment, thus requiring small values of t_d . Using literature data for intracellular diffusion [34] and exchange rates [7] one can show that intracellular water starts displaying the effects of restricted diffusion on a time scale of 1 ms and exchanges with the extracellular component on the time scale of 0.1–1 s. Values of t_d and δ on the time scale of 10 ms is used here as a compromise between maximizing restricted diffusion and minimizing exchange during diffusion encoding. Small values of t_e also reduce the influence of T_2 relaxation which not only leads to lower signal-to-noise, but potentially also introduces systematic errors if T_2 of the two components are not identical.

The information about exchange is contained within the variation of f_e with t_m according to Eq. (7). Accurate estimates of the values of D_e and D_i are of less importance. This means that the range of b -values should be chosen a bit differently from conventional

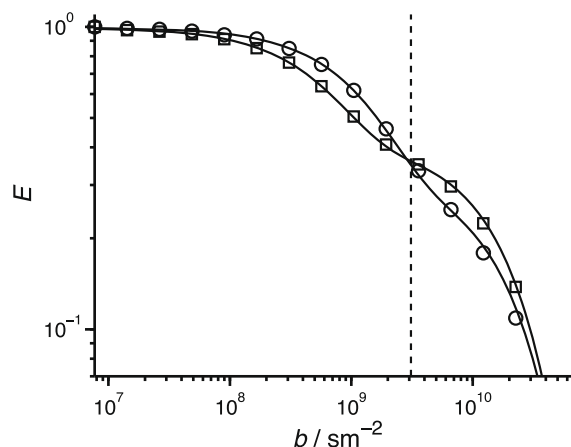


Fig. 2. NMR signal E vs. diffusion weighting b for water in a yeast cell sediment. The data were acquired with the FEXSY pulse sequence using small values of g_f and t_m , thus corresponding to a standard PGSE experiment. Experimental data points for 5 and $32 \text{ }^\circ\text{C}$ are shown as circles and squares, respectively. Fits of Eq. 3 to the data are indicated with solid lines. The dashed vertical line shows the b -value used for the diffusion filter for the FEXSY data in Fig. 3.

PGSE studies typically employing a linear or quadratic sequence of b . For an estimate of f_e it is important to have some data points at $b \ll 1/D_e$, giving the total signal, and some in the range $1/D_e < b < 1/D_i$, yielding the intracellular component. Although higher b -values were used here, it should be pointed out that it is sufficient to use a range of b accessible with standard high-resolution NMR probes and even modern high-gradient clinical MR scanners.

Experimental PGSE data for the yeast cell sediment is shown in Fig. 2. The two exponential components have previously been assigned to extra- and intracellular water based on their respective behavior when varying δ [9,34]. Analysis of the data with Eq. (3) yields $D_e = 7.4 \pm 0.5 \times 10^{-10} \text{ m}^2 \text{ s}^{-1}$ and $D_i = 4.6 \pm 0.4 \times 10^{-11} \text{ m}^2 \text{ s}^{-1}$ for $5.0 \text{ }^\circ\text{C}$, and $D_e = 1.6 \pm 0.1 \times 10^{-9} \text{ m}^2 \text{ s}^{-1}$ and $D_i = 4.7 \pm 0.4 \times 10^{-11} \text{ m}^2 \text{ s}^{-1}$ for $32.0 \text{ }^\circ\text{C}$. D_e is increasing with T as expected for a bulk liquid. The minor variation of D_i with T is consistent with restricted diffusion in a micrometer-scale spherical cavity. For the purpose of this contribution it is sufficient to note that $b = 3.1 \times 10^9 \text{ s m}^{-2}$ for the diffusion filter is an appropriate value to remove the signal from the extracellular component at all investigated temperatures.

4.2. FEXSY experiment and analysis

In Fig. 3(a), an example FEXSY data set is shown. At short t_m the signal decay almost exclusively consists of the intracellular component. With increasing t_m the extracellular component gradually appears.

Eq. (3) with Eq. (7) was globally fitted to the experimental data using a Levenberg–Marquardt least-squares algorithm implemented in Matlab [38]. The following adjustable parameters were used: D_e , D_i , f_e^{eq} , $f_e(0)$, k , and the $b = 0$ signal intensity for each series with different t_m . The variation of the signal-to-noise ratio with t_m was taken into account when evaluating the quality of the fit. From f_e^{eq} and k , the values of k_i and P were calculated with Eqs. (10) and (12). A cell radius of $2.48 \text{ } \mu\text{m}$ was assumed in the latter calculation [34]. Monte Carlo error analysis [39] was used to assess the uncertainty of the fitted parameters.

In order to check that $f_e(t_m)$ obeys Eq. (7), Eq. (3) was individually fitted to each of the data series with different t_m . In these fits, the values of D_e and D_i were constrained to be independent of t_m . A comparison between the two methods of data analysis is shown in Fig. 3(b), indicating that Eq. (7) accurately describes the evolution of $f_e(t_m)$.

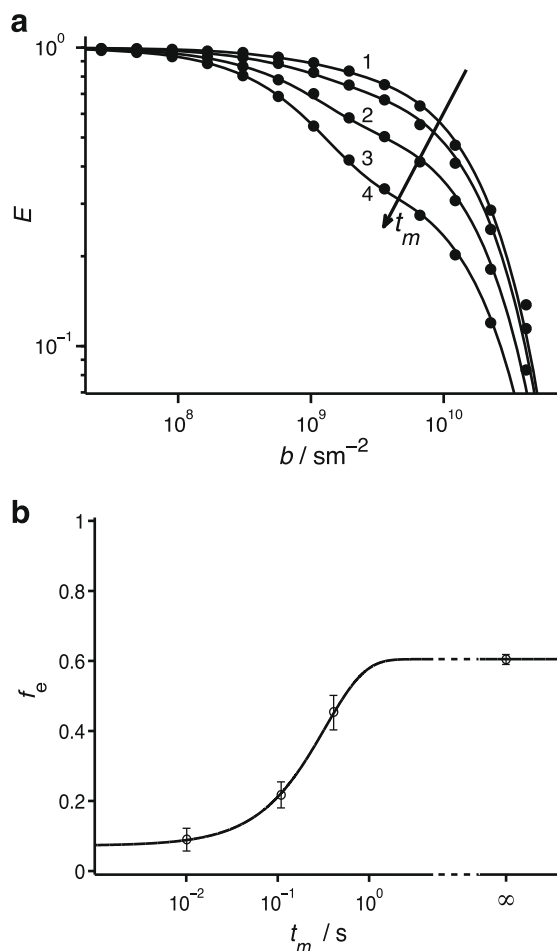


Fig. 3. FEXSY experiment applied to water in a yeast sediment at 25 °C. (a) NMR signal E vs. diffusion encoding b for different mixing times t_m . The circles indicate experimental data points and the lines show the results of a global model fit yielding the effective exchange rate $k = 3.5 \pm 0.4 \text{ s}^{-1}$ and the extracellular fraction at equilibrium $f_e^q = 0.60 \pm 0.008$ (see text for details). The numbers indicate the different experimental series, see Table 1 for parameter details. (b) Extracellular fraction f_e vs. t_m . The circles with error bars (90%-confidence interval) indicate the results of fits of Eq. (3) to each of the series with different t_m in (a). The line is a plot of Eq. (7) using values of k , f_e^q , and $f_e(0)$ obtained from the global fit.

The range of $\tau = 1/k$ that can be measured with reasonable accuracy is set by limitations of the NMR equipment and the values of T_1 . The lower limit of τ is determined by the maximum available gradient strength and the gradient slew rate since δ and t_d have to be much smaller than τ in order to avoid exchange during diffusion encoding. In addition, the time scales for restricted diffusion and exchange have to be well separated to clearly resolve the intra- and extracellular fractions. The FEXSY experiment is thus not appropriate for systems with large and highly permeable cells such as erythrocytes [1,8]. Increasing t_m leads to deteriorating signal-to-noise due to T_1 relaxation, thus setting an upper limit to the value of τ . In order to detect exchange there has to be a significant variation of $f_e(t_m)$ within the window of available t_m , approximately 10 ms to 1 s. Data with effectively infinite t_m can be recorded as described in Section 3 to improve the accuracy for samples with long τ .

4.3. Membrane permeability vs. temperature

As shown in Fig. 4, the cell membrane permeability is increasing and the intracellular lifetime is decreasing with temperature. The values of τ_i range from 0.35 s at 32.0 °C to 1.0 s at 5.0 °C. Our

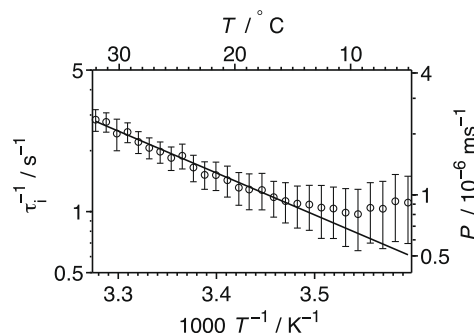


Fig. 4. Intracellular lifetime τ_i and membrane permeability P vs. temperature T for water in yeast cells. Circles with error bars (68.3%-confidence) indicate experimental data from the FEXSY experiment. The solid line shows the result of an Arrhenius analysis yielding the activation energy $E_a = 40 \pm 5 \text{ kJ/mol}$. P is obtained using Eq. (12) and a radius of $2.48 \pm 0.01 \mu\text{m}$ [34]. The influence of the uncertainty in the radius is not included in the calculations of P .

results agree favorably with the study by Labadie et al. [7] who obtained $\tau_i = 0.67 \text{ s}$ (temperature not specified) for rehydrated dry yeast using T_1 -relaxation and paramagnetic doping. It should be noted that comparing the results from different studies is not trivial since the cell properties depend on the yeast strain and the details of sample preparation [40,28].

From an inspection of the Arrhenius plot in Fig. 4, it is clear that a single activation energy E_a cannot describe the variation of P with T . Such behavior is quite common for erythrocytes and has been interpreted as being caused by a phase transition of the membrane lipids or changing conformation and activity of the aquaporins [1]. A non-linear Arrhenius fit, taking into account the varying statistical uncertainty of the data at different T , yields $E_a = 40 \pm 5 \text{ kJ/mol}$. This value is about 2 times higher than those typically observed for erythrocytes [29,1,3], but quite similar to 43 kJ/mol obtained for liquid crystalline egg lecithin vesicles [41]. The aquaporin channels can be presumed to be closed, because of the low intracellular pH caused by the yeast starvation [42], and the cell wall should not be limiting for water transport, since it is very porous [43,44]. These effects leave the plasma membrane permeability as the limiting factor for yeast cell water exchange, which is consistent when comparing the measured E_a with that of a simple phospholipid bilayer.

5. Conclusions

The filter-exchange PGSE sequence proposed here provides a fast and accurate method for determining the intracellular lifetime and membrane permeability of living cells without requiring contrast agents. The demands on the gradients are rather modest, thus making the method possible to implement on high-resolution probes, benchtop NMR systems, and even clinical MR scanners.

Acknowledgment

This work is financially supported by the Swedish Foundation for Strategic Research (SSF) and the Swedish Research Council (VR) through the Linnaeus Center of Excellence on Organizing Molecular Matter (OMM).

References

- [1] G. Benga, Water transport in red blood cell membranes, *Prog. Biophys. Mol. Biol.* 51 (1988) 193–245.
- [2] S. Hohmann, R.M. Bill, G. Kayingo, B.A. Prior, Microbial MIP channels, *Trends Microbiol.* 8 (2000) 33–38.
- [3] P. Agre, Aquaporin water channels (Nobel lecture), *Angew. Chem. Int. Ed.* 43 (2004) 4278–4290.

- [4] P. Hersen, M.N. McClean, L. Mahadevan, S. Ramanathan, Signal processing by the HOG MAP kinase pathway, *Proc. Natl. Acad. Sci. USA* 105 (2008) 7165–7170.
- [5] H.Y. Elmoazzen, J.A.W. Elliott, L.E. McGann, Osmotic transport across cell membranes in nondilute solutions: a new nondilute solute transport equation, *Biophys. J.* 96 (2009) 2559–2571.
- [6] J.A. Dix, A.K. Solomon, Role of membrane proteins and lipids in water diffusion across red cell membranes, *Biochim. Biophys. Acta* 773 (1984) 219–230.
- [7] C. Labadie, J.-H. Lee, G. Větek, C.S. Springer Jr., Relaxographic imaging, *J. Magn. Reson. B.* 105 (1994) 99–112.
- [8] T. Conlon, R. Outhred, Water diffusion permeability of erythrocytes using an NMR technique, *Biochim. Biophys. Acta* 288 (1972) 354–361.
- [9] C. Malmberg, M. Sjöbeck, S. Brockstedt, E. Englund, O. Söderman, D. Topgaard, Mapping the intracellular fraction of water by varying the gradient pulse length in q -space diffusion MRI, *J. Magn. Reson.* 180 (2006) 280–285.
- [10] J. Andrasko, Water diffusion permeability of human erythrocytes studied by a pulsed gradient NMR technique, *Biochim. Biophys. Acta* 428 (1976) 304–311.
- [11] P. van Zijl, C.T.W. Moonen, P. Faustino, J. Pekar, O. Kaplan, J.S. Cohen, Complete separation of intracellular and extracellular information in NMR spectra of perfused cells by diffusion-weighted spectroscopy, *Proc. Natl. Acad. Sci. USA* 88 (1991) 3228–3232.
- [12] A.R. Waldeck, P.W. Kuchel, A.J. Lennon, B.E. Chapman, NMR diffusion measurements to characterise membrane transport and solute binding, *Prog. NMR Spectrosc.* 30 (1997) 39–68.
- [13] J. Kärger, NMR self-diffusion studies in heterogeneous systems, *Adv. Colloid Interface Sci.* 23 (1985) 129–148.
- [14] P.T. Callaghan, *Principles of Nuclear Magnetic Resonance Microscopy*, Oxford University Press Inc., New York, 1991.
- [15] W.S. Price, A.V. Barzykin, K. Hayamizu, M. Tachiya, A model for diffusive transport through a spherical interface probed by pulsed-field-gradient NMR, *Biophys. J.* 74 (1998) 2259–2271.
- [16] J.-H. Lee, C.S. Springer Jr., Effects of equilibrium exchange on diffusion-weighted NMR signals: the diffusographic shutter-speed, *Magn. Reson. Med.* 49 (2003) 450–458.
- [17] C.S. Johnson Jr., Effects of chemical exchange in diffusion-ordered 2D NMR spectra, *J. Magn. Reson. A* 102 (1993) 214–218.
- [18] P.T. Callaghan, I. Fufo, Diffusion–diffusion correlation and exchange as a signature for local order and dynamics, *J. Chem. Phys.* 120 (2004) 4032–4038.
- [19] Y.-Q. Song, L. Venkataramanan, M.D. Hürlimann, M. Flaum, P. Frulla, C. Straley, $T_1 - T_2$ Correlation spectra obtained using a fast two-dimensional Laplace inversion, *J. Magn. Reson.* 154 (2002) 261–268.
- [20] J. Jeener, B.H. Meier, P. Bachmann, R.R. Ernst, Investigation of exchange processes by two-dimensional NMR spectroscopy, *J. Chem. Phys.* 71 (1979) 4546–4553.
- [21] M. Goldman, L. Shen, Spin–spin relaxation in LaF_3 , *Phys. Rev.* 114 (1966) 321–331.
- [22] M.A. Voda, D.E. Demco, A. Voda, T. Schaubert, M. Adler, T. Dabisch, A. Adams, M. Baias, B. Blümich, Morphology of thermoplastic polyurethans by H spin diffusion in NMR, *Macromolecules* 39 (2006) 4802–4810.
- [23] D. Topgaard, O. Söderman, Diffusion of water absorbed in cellulose fibers studied with ^1H NMR, *Langmuir* 17 (2001) 2694–2702.
- [24] D. Topgaard, O. Söderman, Self-diffusion of nonfreezing water in porous carbohydrate polymer systems studied with NMR, *Biophys. J.* 83 (2002) 3596–3606.
- [25] N. Campbell, J. Reece, L. Mitchell, *Biology*, fifth ed., Benjamin/Cummings, Meulo Park, 1999.
- [26] W.H. Mager, J. Winderickx, Yeast as a model for medical and medicinal reserach, *Trends Pharmacol. Sci.* 26 (2005) 265–273.
- [27] M. Menacho-Marquez, J.R. Murguía, Yeast on drugs: *Saccharomyces cerevisiae* as a tool for anticancer drug research, *Clin. Transl. Oncol.* 9 (2007) 221–228.
- [28] G. Kayingo, R.M. Bill, G. Calamita, S. Hohmann, B.A. Prior, Microbial water channels, *Curr. Top. Memb.* 51 (2001) 335–370.
- [29] T. Conlon, R. Outhred, The temperature dependence of erythrocyte water diffusion permeability, *Biochim. Biophys. Acta* 511 (1978) 408–418.
- [30] P. Stilbs, Fourier transform pulsed-gradient spin-echo studies of molecular diffusion, *Prog. Nucl. Magn. Reson. Spectrosc.* 19 (1987) 1–45.
- [31] W.S. Price, Pulsed-field gradient nuclear magnetic resonance as a tool for studying translational diffusion: Part1. Basic theory, *Concepts Magn. Reson.* 9 (1997) 299–336.
- [32] B. Blümich, *NMR Imaging of Materials*, Oxford University Press, Oxford, 2000.
- [33] R. Kimmich, *NMR: Tomography, Diffusometry, Relaxometry*, Springer-Verlag, Berlin, 1997.
- [34] I. Åslund, D. Topgaard, Local self-diffusion coefficient of intracellular water determined with NMR, *J. Magn. Reson.*, submitted for publication.
- [35] J.S. Murday, R.M. Cotts, Self-diffusion coefficient of liquid lithium, *J. Chem. Phys.* 48 (1968) 4938–4945.
- [36] S. Zumdahl, S. Zumdahl, *Chemistry*, fifth ed., Houghton Mifflin Company, Boston, 2000.
- [37] A.V. Barzykin, K. Hayamizu, W.S. Price, M. Tachiya, Pulsed-field-gradient NMR of diffusive transport through a spherical interface into an external medium containing a relaxation agent, *J. Magn. Reson. A* 114 (1995) 39–46.
- [38] Matlab v. 7.5, The MathWorks, Natick, MA.
- [39] J.S. Alper, R.I. Gelb, Standard errors and confidence intervals in nonlinear regression: comparison of monte carlo and parametric statistics, *J. Phys. Chem.* 90 (1990) 4747–4751.
- [40] Y.-S. Hong, K.-J. Suh, S.-W. Yoon, V. Skirda, V. Volkov, C.-H. Lee, Effect of heat treatment on water permeability of yeast cells as measured by pulsed field gradient (PFG) NMR spectroscopy, *Food Sci. Biotechnol.* 13 (2004) 586–590.
- [41] C. Lipschitz-Farber, H. Degani, Kinetics of water diffusion across phospholipid membranes, *Biochim. Biophys. Acta* 600 (1980) 291–300.
- [42] K. Hedfalk, S. Törnroth-Horsefield, M. Nyblom, U. Johanson, P. Kjellbom, R. Neutze, Aquaporin gating, *Curr. Opin. Struct. Biol.* 16 (2006) 447–456.
- [43] M. Osumi, The ultrastructure of yeast: cell wall structure and formation, *Micron* 29 (1998) 207–233.
- [44] P.N. Lipke, R. Ovalle, Cell wall architecture in yeast: new structure and new challenges, *J. Bacteriol.* 180 (1998) 3735–3740.